J Fluoresc (2015) 25:1739–1747
DOI 10.1007/s10895-015-1660-8

ORIGINAL ARTICLE

Relaxation Photoprocesses in a Crowned Styryl Dye and its Metal Complex

Michael V. Rusalov[1] · Boris M. Uzhinov[1] · Sergey I. Druzhinin[2] · Vladimir L. Ivanov[1] · Michael Ya. Melnikov[1] · Sergey P. Gromov[3] · Sergey K. Sazonov[3] · Michael V. Alfimov[3]

Received: 7 May 2015 / Accepted: 14 September 2015 / Published online: 26 September 2015

Abstract The effects of solvent and crown-ether moiety on spectral properties of pyridinium styryl dye were studied by steady-state absorption and fluorescent spectroscopy. Analysis of viscosity and polarity effects on fluorescence quantum yield and Stokes shift permitted us to suggest that there is a two stage process of excited state relaxation. The macrocyclic moiety has a little influence on the first stage of relaxation, which manifests itself in a magnitude of Stokes shift, but suppresses considerably the second stage, which manifests itself in a magnitude of fluorescence quantum yield. The metal complex shows an additional stage of excited state relaxation, namely, photorecoordination of metal cation within the macrocyclic cavity.

Keywords Crown ether · Styryl dye · Complex formation · Photorecoordination · Molecular rotor

Introduction

Excited singlet states of aromatic molecules, which were formed as a result of fast vibrational relaxation of an initial Frank-Condon state, are capable of undergoing further relaxation processes with retaining of electronic excitation. One of such processes is the process of conformational rearrangement of the light absorbed molecule, i.e., of the structural relaxation [1].

The structural relaxation leads to changes in the geometry of excited molecules, which as a rule manifest themselves in the rotation of its fragments relative to each other [2–5]. In some cases instead of the mutual rotation, a change in pyramid-like formation takes place in one of heteroatoms, an increase in pyramidalization degree [6] as well as flattening of the structure being possible [7]. The structural relaxation manifests experimentally itself in anomalous Stokes shift of the relaxation product [4, 8, 9], in continuous shift or widening of fluorescent spectra [10–13], in fluorescence anisotropy [14–16], in considerable dependence of fluorophore luminescent properties on solvent viscosity and pressure [6, 10, 17]. At the same time, the attributes of structural relaxation mentioned above should be analyzed along with other relaxation processes which occur also for rigid molecules, for instance, rotational depolarization, solvent relaxation, and so on.

When the product of structural relaxation does not fluoresce, the relaxation process results in fluorescence quenching [4, 18].

As a consequence of the determinative influence of the local environment on the structural relaxation, organic fluorophores are used as optic sensors (molecular rotors) for measurement of local viscosity in chemical and biological objects, for monitoring of polymerization, aggregation and conformation analysis of proteins, viscous flow of liquids [19].

The most important class of molecular rotors is a group of compounds, the molecules of which being electronically excited, are capable of passing into a Twisted Intramolecular Charge Transfer (TICT) state [20–25]. The excited molecules of these compounds undergo adiabatic intramolecular reaction, which consists in charge transfer from a donor

✉ Michael V. Rusalov
mvrusalov@yandex.ru

[1] Department of Chemistry, MV Lomonosov Moscow State University, Leninskie Gory 1, 119991 Moscow, Russian Federation

[2] Universität Siegen, Physikalische Chemie, Adolf-Reichwein-Str. 2, 57076 Siegen, Germany

[3] Photochemistry Center, Russian Academy of Sciences, Novatorov 7a, 119421 Moscow, Russian Federation

fragment to an acceptor one and their mutual rotation. TICT state is characterized by a weak degree of π-orbital overlapping of donor and acceptor fragments. Thus, the radiative transition is prohibited. That is why in non-rigid medium these compounds have low fluorescent quantum yield or anomalous Stokes shift [20–25]. In some cases, when radiative deactivation is carried out both from Local Excited (LE) state and from TICT state, the dual fluorescence is observed. The shortwave band corresponds to the LE state, while the longwave band corresponds to the TICT state [2, 5].

Styryl and cyanine dyes are widely used as molecular optic sensors and photoswitchable devices [26–29], for information recording on optic disks, as laser dyes and non-linear optic media, sensitizers in photography, in solar power engineering, in biology and medicine, in textile industry [30–32].

Stylbazolium salt derivatives are intensively studied because of their high photostability, related with low quantum yield of photoinduced *trans-cis-* isomerization, as well as with strong dependence of fluorescence intensity on solvent viscosity. These results open up perspectives for their practical application as local viscosity sensors [33–37]. A possibility of practical use was shown of stylbazolium derivatives for spatial visualization of intracellular microviscosity [38, 39].

The purpose of the present paper was to study the effects of crown-ether substituent on relaxation of excited molecules of a pyridinium styryl dye in solvents of various viscosity and polarity.

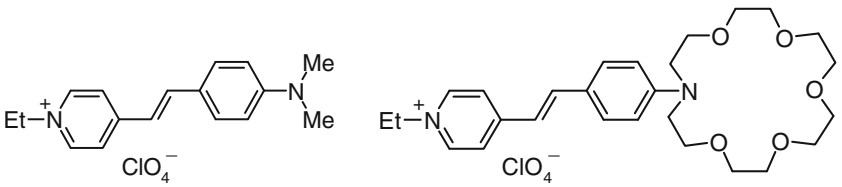

1a **1b**

Results and Discussion

Fluorescence of pyridinium styryl dye **1a** in non-viscous organic solvents is usually characterized by low quantum yield (1–3 %) and large magnitude of Stokes shift (about 4000–5000 cm^{-1}). As is seen from the Table 1, fluorescence quantum yield of **1a** decreases in general as solvent polarity increases. For example, in case of solvents such as ethyl acetate, butyronitrile, acetonitrile, water, the drop of fluorescence quantum yield (φ is equal to 0.033, 0.023, 0.0069 and 0.0013, respectively) is observed with an increase in solvent dielectric permeability (ε is equal to 6, 20, 36 and 78, respectively [40]). At the same time, the compound **1a** fluoresces intensively in glycerol (φ=0.59), which is a polar (ε=43) and viscous solvent.

Similar to stilbene and its derivatives [41], many styryl dyes undergo photoinduced *trans-cis*-isomerization and the reverse process due to rotation around double bond upon light irradiation [26, 27]. However, some of the structures possess high photostability and low photoisomerization quantum yield. At this case, the main channel of radiationless deactivation of excited molecules is considered to be formation of twisted TICT state [33–39, 42, 43].

The following facts point to the possibility of TICT state formation in stilbazolium salts: low fluorescence quantum yield of a pre-twisted model compound in polar solvents (0.0005) [33], 20-fold increase in lifetime (from 85 ps to 2 ns) of a model compound with fixed rotation around formal ordinary bonds [34], a decrease in fluorescence quantum yield as solvent polarity increases [35, 37], dual fluorescence of some crowned stilbene [44, 45], an increase in fluorescence and *trans-cis*-isomerization quantum yield upon complex formation of crowned dyes with metal cations, whose electrostatic field suppresses charge transfer [42, 43].

The twisted state is formed by mutual rotation of molecular fragments relative to each other around central formal single or double bonds. In the latter case *trans-cis*-isomerization does not occur. According to the paper [33], upon the formation of TICT state of *o*, *m*- and *p*-(dimethyl)-stilbazolium, the rotation occurs around all three central bonds. Later it was proven by the model compound method that the formation of TICT state by central double bond is impossible [34]. Its formation was accounted for by the rotation around two central single bonds [34] or around only one central single bond with an aniline fragment [36].

Thus, the decrease in fluorescence quantum yield of **1a**, as solvent polarity increases, can be explained by the stabilization of non-fluorescing TICT state. In its turn, solvent viscosity increase suppresses the rotation of molecular fragments relative to each other. For instance, fluorescence quantum yield of **1a** in hexanol and in glycerol exceeds 10–20 times of that one in ethanol and butyronitrile. In case of glass matrices, the internal rotation, which is necessary for TICT state formation, is suppressed completely, that is why fluorescence quantum yield of **1a** is equal to unity within the experimental accuracy.

Table 1 Maxima of absorption (λ_a) and fluorescence (λ_f and $\tilde{\nu}_f$), fluorescence quantum yields (φ) and Stokes shifts ($\Delta\tilde{\nu}_s$) of compounds **1a**, **1b**, **1a**·H^+ and **1b**·Ba^{2+} in various solvents at 295 K and in some rigid matrices

Compound	Solvent	λ_a, nm	λ_f, nm	$\tilde{\nu}_f \cdot 10^{-3}$, cm^{-1}	φ	$\Delta\tilde{\nu}_s \cdot 10^{-3}$, cm^{-1}
1a	Ethyl acetate	463.6	603	16.5	0.033	5.1
	Dichloromethane	519.9	610	16.3	0.19	2.9
	Butyronitrile	478.1	620	16.0	0.023	4.9
	Butyronitrile, 77 K	482.9	536	18.6	1.0±0.15	2.1
	Acetonitrile	469.9	620	16.0	0.0069	5.2
	Hexanol	489.1	609	16.4	0.22	4.1
	Butanol	487.0	610	16.4	0.074	4.2
	Ethanol	481.4	611	16.3	0.033	4.5
	Ethanol, 77 K	489.3	543	18.3	1.0±0.15	2.1
	Glycerol	481.0	611	16.2	0.59	4.6
	Water	447.8	609	16.4	0.0013	6.0
	PMMA	473.8	592	16.8	1.0±0.15	4.3
	PMMA, 77K	474.6	572	17.4	1.0±0.15	3.7
1b	Ethyl acetate	472.9	607	16.4	0.12	4.8
	Dichloromethane	523.6	614	16.2	0.16	2.9
	Butyronitrile	485.1	620	16.0	0.056	4.6
	Butyronitrile, 77 K	487.3	534	18.7	1.0±0.15	1.9
	Acetonitrile	476.0	620	16.0	0.021	5.0
	Hexanol	493.7	610	16.3	0.35	3.9
	Butanol	492.1	611	16.2	0.18	4.1
	Ethanol	485.4	613	16.2	0.088	4.4
	Ethanol, 77 K	493.0	548	18.2	1.0±0.15	2.1
	Glycerol	482.0	607	16.4	1.00	4.4
	Water	455.6	608	16.3	0.015	5.6
	PMMA	481.7	597	16.6	1.0±0.15	4.1
	PMMA, 77K	482.8	581	17.2	1.0±0.15	3.6
1a·H^+	Butyronitrile	331.0	428	22.7	0.0041	7.5
	Butyronitrile, 77 K	335.5	390	25.5	0.74±0.15	4.3
1b·Ba^{2+}	Butyronitrile	361.1	604	16.5	0.11	11.2
	Butyronitrile, 77K	389.4	504	19.7	1.0±0.15	6.0
	Acetonitrile	360.8	604	16.5	0.12	11.2
	Ethanol	361.1	596	16.7	0.15	11.0
	Ethanol, 77 K	369.3	512	19.4	1.0±0.15	7.7
	PMMA	363.0	530	18.6	0.71±0.15	9.0
	PMMA, 77 K	379.4	491	20.0	1.0±0.15	6.4

The introduction of the voluminous crown-ether substituent into the molecule of **1a** also suppresses the formation of TICT state. That is why fluorescence quantum yield of the compound **1b** in various solvents is, as a rule, higher than in case of compound **1a**. The electrostatic field of a metal cation and a solvent shell of the second coordination sphere suppress even to a greater extend the mutual rotation and favor an increase in fluorescence quantum yield. So, fluorescence quantum yields of the compounds **1a**, **1b** and **1b**·Ba^{2+} in acetonitrile are equal to 0.0069, 0.021 and 0.12, respectively.

The compound **1a** shows noticeable solvatochromism, which, however, is not a simple monotonous function of dielectric permeability ε, Lippert's solvent function $f(\varepsilon, n)$ [46] and the empirical polarity scale E_T^{30} (Table 2). For example, ε, $f(\varepsilon, n)$ and E_T^{30} (6, 9, 20, 36, 78; 0.20, 0.22, 0.27, 0.30, 0.32 and 38, 41, 43, 46, 63 kcal·mol^{-1}, respectively [40]) for such solvents as ethyl acetate, dichloromethane, butyronitrile, acetonitrile and water increase monotonously, whereas the maximum of absorption spectra changes in a non-monotonous way (464, 520, 478, 470, 448 nm, respectively). This can be accounted for by the difference between macroscopic and

Table 2 Viscosity (η) and the empirical polarity scale (E_T^{30}) of various solvents under normal conditions [40]

Solvent	E_T^{30}, kcal·mol^{-1}	η, cP
Ethyl acetate	38.1	0.426
Dichloromethane	41.4	0.411
Butyronitrile	43.0	0.549
Acetonitrile	46.0	0.341
Hexanol	49.4	4.590
Butanol	50.2	2.593
Ethanol	51.9	1.214
Glycerol	57.0	1390
Water	63.1	0.894

local dielectric permeability. In case of E_T^{30}, this means that the given empirical scale does not describe exactly local polarity for the systems in question and should be corrected.

The study of concentration dependencies of **1a** fluorescence in dichloromethane showed the absence of dimerization and specific interaction with the solvent. The invariability of fluorescence quantum yield of **1a** upon 20-times dilution shows that dimerization does not occur. The monotonous shift of **1a** maximum in dichloromethane-butyronitrile mixture up to 0.8 mole fraction shows that strong complexes between solvent and solute are not formed.

At the same time, solvent polarity effects weak on **1a** fluorescence maximum, which is located near 610 nm. This fact points to small polarity of the excited state of **1a**, which emits light [35, 36]. The shift of **1a** absorption maximum towards shortwave band, as solvent polarity increases, also points to small polarity of the excited state [35, 36].

Since Stokes shift considerably decreases (by ~3000 cm^{-1}) in glassed butyronitrile and ethanol solutions of **1a**, then there exists a relaxation process in liquid solutions which is suppressed in glassed media. The authors [34] relate this phenomenon with the fast process of solvent relaxation, which leads to the Relaxed Solvate Shell (RSS) state with re-orientated solvent shell. The RSS formation occurs with the characteristic times 20 ps in ethanol and 500 ps in more viscous decanol, which is much shorter than lifetime of the excited states (80 and 900 ps for the styryl dye with non-fixed single bonds, 1400 and 2400 ps for the dye with fixed single bonds, respectively). The solvent re-orientation manifests itself in dynamic Stokes shift which increases by 1600 cm^{-1} for the times mentioned above.

The formation of RSS state is practically completely suppressed in glassed butyronitrile and ethanol at 77K, it is insignificantly suppressed in polymeric PMMA matrix at room temperature and somewhat better upon cooling to 77K. The small efficiency of PMMA matrix in relaxation suppressing may be caused by internal voids. It is known that logarithm of effective viscosity is in inverse proportion to free volume [19]. Viscosity of liquid solvents such as glycerol is not high enough for noticeable suppressing of the given relaxation process. It is evident from the position of **1a** fluorescence maximum in butyronitrile and ethanol at 77 K, in PMMA at 295 K and 77 K, in glycerol at 295 K (536, 543, 592, 572 and 611 nm, respectively).

The introduction of the macrocycle into the **1a** molecule leads to a small decrease in Stokes shift values (about by 200 cm^{-1}, i.e., by 4 %).

The complex formation of **1b** with the cation Ba^{2+} in butyronitrile causes a great hypsochromic shift (6400 cm^{-1}, Fig. 1), which is related with withdrawing the crown-ether aminogroup from conjugation of molecular π-system due to the binding of amino group by metal cation. At the same time, the shortwave shift of fluorescence maximum is small (430 cm^{-1}). Such difference in behavior of absorption and fluorescence spectra points to the additional relaxation process, namely, to photorecoordination of metal cation in crown-ether cavity [44, 45, 47–53].

Photorecoordination together with other relaxation processes result in anomalous Stokes shift of the metal complex (about 11,000 cm^{-1}). Although photorecoordination requires a considerable rearrangement of macrocycle geometry, and the change in mutual location of crown-cycle relative to chromophoric molecular part from orthogonal to complanar, and also the inclusion of several solvent molecules into the first coordination sphere of metal cation [49–52], it is known that photorecoordination is not completely suppressed in rigid media [54, 55]. Accordingly, Stokes shift of **1b**·Ba^{2+} remains high (6000–8000 cm^{-1}) even in rigid matrices at 77K, which indicates that photorecoordination is not suppressed noticeably under the given conditions.

Since upon the protonation of the compound **1a** at the nitrogen atom of dimethylamino group, its withdrawal takes place from conjugation, quite similar to that which takes place

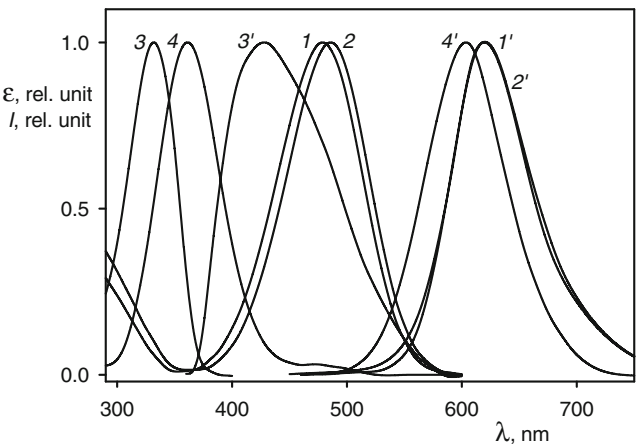

Fig. 1 Normalized spectra of absorption (*1–4*) and fluorescence (*1′–4′*) of the compounds **1a** (*1, 1′*), **1b** (*2, 2′*), **1a**·H^+ (*3, 3′*) and **1b**·Ba^{2+} (*4, 4′*) in butyronitrile at 295 K

upon complex formation of **1b** with barium cation, it was interesting to compare Stokes shifts of **1a**·H^+ и **1b**·Ba^{2+} in various conditions. The Table 1 shows that Stokes shift of **1a**·H^+ in butyronitrile is noticeably less the that for **1b**·Ba^{2+} at room temperature (by 3700 cm^{-1}) as well as at 77K (by 1700 cm^{-1}). It can be explained by the fact that in case of **1a**·H^+ photorecoordination and proton phototransfer do not take place. Thus, the compound **1a**·H^+ may be regarded as a model compound for **1b**·Ba^{2+}, in which photorecoordination is excluded.

The difference in the position of absorption spectrum maxima of **1a**·H^+ and **1b**·Ba^{2+} in butyronitrile (2500 cm^{-1}) is considerably smaller than the similar value for fluorescence spectra both at room temperature (6800 cm^{-1}) and at 77 K (5800 cm^{-1}). As it was mentioned above, this fact is caused by an additional relaxation process in **1b**·Ba^{2+}, namely, by photorecoordination of metal cation.

Thus, the basic relaxation processes in the metal complex excited molecule can be described by the following scheme:

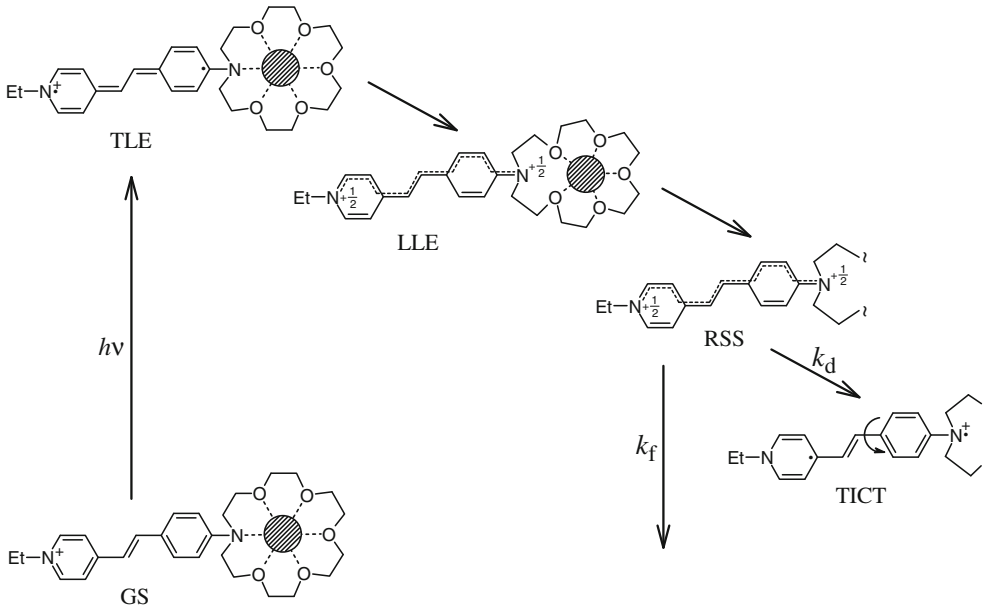

The light absorption by the molecule of the complex in Ground State (GS) leads to the Tight Local Excited (TLE) state. Further, due to the fast disruption of coordination bond between nitrogen atom and metal cation and due to displacement of barium cation from its equilibrium position, the Loose Local Excited (LLE) state is formed. After that, solvent relaxation leads to Relaxed Solvate Shell (RSS) state. The radiative deactivation (k_f) and radiationless deactivation (k_d), caused by the formation of non-fluorescent TICT state, are the main channels of RSS transformation.

For monomolecular reactions, which are accompanied by internal rotation, the Kramer's model allows to describe quantitatively the influence of temperature, polarity and viscosity of the solvent on the rate constant [56].

According to this model, the rate constant k of monomolecular reaction can be expressed as

$$k = \frac{A}{\eta^{\alpha}} \exp\left(-\frac{E_a}{RT}\right), \quad (1)$$

where A is a constant, which does not depend on temperature and viscosity, η is solvent viscosity, α is a power index which is equal to the unity for higher viscosities, E_a is an activation energy.

Ab initio quantum mechanical calculations point to a barrierless rotation around a formal single bond at phenylazacrown and benzoazacrown moieties as the main channel of radiationless deactivation of crowned styryl dyes [51, 52]. However, since fluorescence quantum yield of stilbazolium salts significantly depends on solvent polarity [35, 37], it can be assumed that the reaction of TICT state formation has a potential barrier, which decreases as solvent polarity increases. According [57], the dependence of potential barrier of TICT state formation E_a on solvent polarity can be express as:

$$E_a = E_0 - \beta\left(E_T^{30} - 30\right), \quad (2)$$

where E_0 is a height of the potential barrier in hexane, E_T^{30} is an empirical solvent polarity, which is equal to 30 kcal/mol for hexane, β is a coefficient. Assuming that TICT state formation is a main channel of deactivation of excited molecules and using the expression (2), the expression (1) can be transformed into

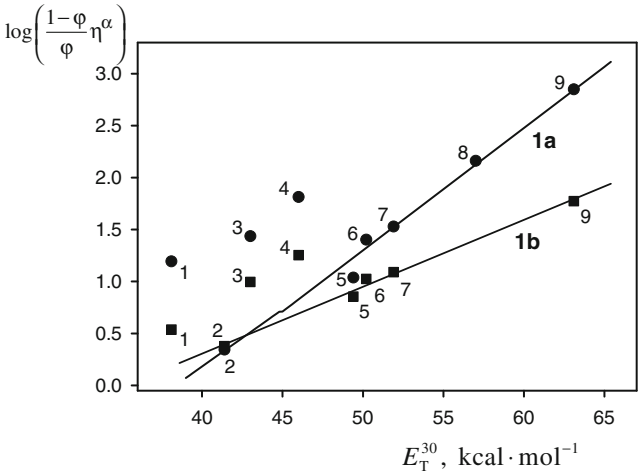

Fig. 2 Correlation between fluorescence quantum yield (φ) of the compounds **1a** and **1b**, viscosity (η) and polarity (E_T^{30}) at 295 K. Numbers represent solvents: ethyl acetate (1), dichloromethane (2), butyronitrile (3), acetonitrile (4), hexanol (5), butanol (6), ethanol (7), glycerol (8), water (9)

$$\frac{1-\varphi}{\varphi} = \frac{A'}{\eta^{\alpha}} \exp\left(\frac{\beta E_T^{30}}{RT}\right), \tag{3}$$

or

$$\ln\left(\frac{1-\varphi}{\varphi}\eta^{\alpha}\right) = \ln A' + \frac{\beta E_T^{30}}{RT}, \tag{4}$$

where A' is $A\exp[-(E_0+30\beta)/RT]$ and does not depend on solvent.

When the empirical scale of polarity E_T^{30} is used in coordinates of the Eq. (4), the experimental points are divided into two groups (Fig. 2). The first group includes proton solvents and dichloromethane, the data of which are satisfactorily described by the Eq. (4) with α and β parameters shown in the Table 3. The second group includes ethyl acetate and nitriles, the data of which fall out of the general dependence (Fig. 2). This means that the parameter E_T^{30} is not universal enough for describing the systems under study. Together with the empirical scale of polarity E_T^{30}, an another measure of local solvent polarity is also Stokes shift $\Delta\tilde{\nu}_s$ [37]. The use of Stokes shift as a function of solvent polarity allowed to include the data on acetonitrile and butyronitrile in the general dependence according to the Eq. (4) with satisfactory correlations (r=0.96–0.98) (Fig. 3). Further increase in the number of solvents included in correlation can be obtained by using a mixed function of polarity $f\left(\Delta\tilde{\nu}_s, E_T^{30}\right)$, which can be expressed as

$$f\left(\Delta\tilde{\nu}_s, E_T^{30}\right) = x\Delta\tilde{\nu}_s + (1-x)E_T^{30}, \tag{5}$$

where x is a parameter to be optimized.

The Fig. 4 shows the correlation among fluorescence quantum yield (φ), Stokes shift $(\Delta\tilde{\nu}_s)$ of compounds **1a** and **1b**, viscosity (η) and polarity (E_T^{30}) of the medium at 295 K (Table 2) using expressions (4) and (5). The best fit x parameter is x=0.81±0.04 for the compound **1a** and x=0.69±0.12 for the compound **1b**.

Proceeding from the value β=0.13 for the compound **1a**, when the scale of polarity (5) is used, and assuming E_a~0 for the TICT state formation in water, the values E_a=1.5 kcal/mol in dichloromethane and E_a=0.6–0.9 kcal/mol in other solvents were obtained.

The dependence of fluorescence quantum yield of the compounds **1a** and **1b** on the composition of ethanol-glycerol mixture was studied in order to verify the expression (3). The given mixture retains approximate the same polarity because values of E_T^{30} for ethanol and glycerol are close (52 and 57 kcal/mol, respectively) and the Stokes shifts of the compounds **1a** and **1b** in these solvents are identical despite of one thousand-fold difference in their viscosities.

In this case, a linear dependence between logarithms of (1–φ)/φ and viscosity η was expected. The Fig. 5 shows the dependence of fluorescence quantum yield of the compounds **1a** and **1b** on the viscosity of ethanol-glycerol mixture, calculated from the percentage [58]. A satisfactory correlation is observed with best fit parameters α=0.56±0.02 for the compound **1a** and α=0.72±0.03 for the compound **1b**. These estimates of the parameter α are in agreement with those ones found above within two standard deviations. A higher value of

Table 3 Optimal values of α and β parameters in the Eq. (4) for the compounds **1a** and **1b**, the number of points N in the regression and the correlation coefficient r when using the empirical scale E_T^{30}, Stokes shift $\Delta\tilde{\nu}_s$ and their combination $f\left(\Delta\tilde{\nu}_s, E_T^{30}\right)$ as a polarity function

	E_T^{30}		$\Delta\tilde{\nu}_s$		$f\left(\Delta\tilde{\nu}_s, E_T^{30}\right)$	
	1a	**1b**	**1a**	**1b**	**1a**	**1b**
α	0.74±0.03	0.89±0.05	0.55±0.07	0.76±0.10	0.67±0.05	0.97±0.13
β	0.069±0.004	0.037±0.002	0.16±0.02	0.10±0.01	0.13±0.01	0.07±0.01
N	6	5	8	7	9	8
r	0.994	0.996	0.96	0.98	0.98	0.96

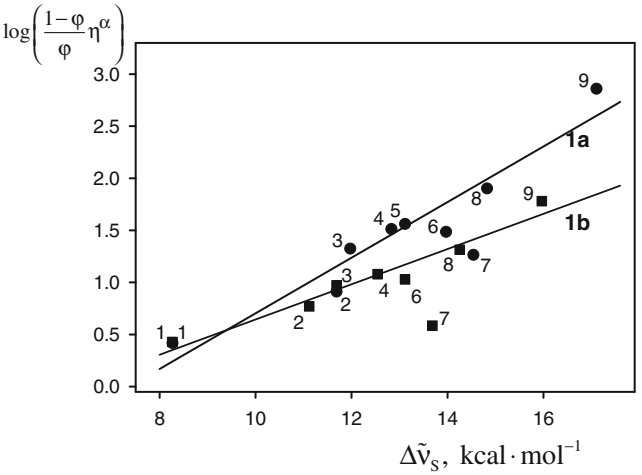

Fig. 3 Correlation between fluorescence quantum yield (φ), Stokes shift ($\Delta\tilde{\nu}_s$) of the compounds **1a** and **1b**, viscosity (η) at 295 K. Numbers represent solvents: dichloromethane (1), hexanol (2), butanol (3), ethanol (4), glycerol (5), butyronitrile (6), ethyl acetate (7), acetonitrile (8), water (9)

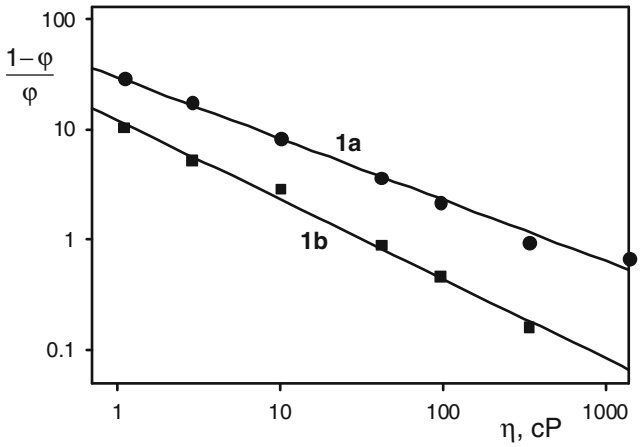

Fig. 5 Dependence of fluorescence quantum yield (φ) of the compounds **1a** and **1b** on viscosity (η) of the ethanol-glycerol mixture at 295 K

the parameter α for the compound **1b** as compared to the compound **1a** points to a lesser slipping of voluminous crown-ether substituent in Kramer's model.

Experimental

The compounds **1a** (4-{(E)-2-[4-(dimethylamino)phenyl]-1-ethenyl}-1-ethylpyridinium perchlorate) and **1b** (4-{(E)-2-[4-(1,4,7,10,13-pentaoxa-16-azacyclooctadecane-16-yl)phenyl]-1-ethenyl}-1-ethylpyridinium perchlorate) were synthesized as was described earlier [59, 60]. Absorption spectra were recorded on "Shimadzu UV–3100" spectrophotometer, fluorescence spectra were recorded on "Elumin–2M". Fluorescence quantum yields were determined by comparison of squares (*S*) under corrected fluorescence spectra of the substances under study and the standards, taking into account for the solvent refractive index (*n*) [61] as follows:

$$\varphi_2 = \frac{S_2 n_2^2}{S_1 n_1^2}\varphi_1 \qquad (6)$$

The solution of quinine sulfate in 1 N sulfuric acid (φ= 0.546) [62] was used as a primary standard. The solution of coumarin-522 in acetonitrile was used as a secondary standard, whose fluorescence quantum yield, determined by the primary standard, is equal to 0.92±0.01 at the presence of air oxygen and 1.00±0.01 at argon atmosphere. These values are in agreement with the value 1.0±0.1 for various solvents [18].

Fluorescence spectra at 77 K were recorded upon cooling samples by liquid nitrogen in quartz Dewar vessel. The solutions of radiation-stitched PMMA in acetone were used for preparation of polymer films. The solvents, checked for absence of fluorescence, were used for preparation of dye solutions: acetone, acetonitrile, butanol, butyronitrile, hexanol, glycerol, dichloromethane, ethanol, ethyl acetate.

Ethanol was dried by distillation over CaH_2. Ethyl acetate and dichloromethane were distilled over K_2CO_3 to remove acid traces. Other solvents were used without further purification. Barium perchlorate was dried in vacuum at temperature 220 °C.

The protonation of the compound **1a** at nitrogen atom of dimethylamino group was performed with trifluoroacetic acid (10^{-2} M), distilled over sulfuric acid. The complex formation of the compound **1b** with Ba^{2+} cation was performed with crystalline barium perchlorate (10^{-2} M). The addition of barium perchlorate to the solution of **1a** at the same concentration does not practically affect the position of absorption and fluorescence maxima, only slightly increasing the fluorescence intensity (by 2 %).

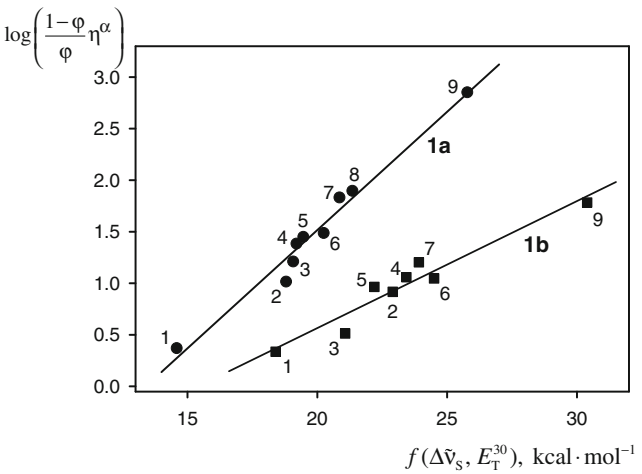

Fig. 4 Correlation between fluorescence quantum yield (φ), Stokes shift ($\Delta\tilde{\nu}_s$) of the compounds **1a** and **1b**, viscosity (η) and polarity (E_T^{30}) at 295 K. Numbers represent solvents: dichloromethane (1), hexanol (2), ethyl acetate (3), butanol (4), butyronitrile (5), ethanol (6), acetonitrile (7), glycerol (8), water (9)

Conclusion

Thus, using the method of steady-state absorption and fluorescence spectroscopy, the relaxation processes of electron-excited molecules of pyridinium styryl dye **1a** and its crowned analog **1b**, were studied. An assumption was made that the relaxation process includes at least two stages. The first stage is the formation of low-polar fluorescing RSS-state, which later at the second stage is transformed into non-fluorescing TICT state. The TICT state formation is a viscosity and polarity dependent process of structural relaxation. The third preliminary stage, namely, photorecoordination of metal cation in macrocycle cavity, is observed in the metal complex **1b**·Ba^{2+}. This stage transforms tight TLE state into loose LLE state. The additional relaxation process of photorecoordination results in anomalous Stokes shift (about 11,000 cm^{-1}). The formation of TICT state can be effectively suppressed in solvents with high viscosity such as hexanol and glycerol, in this case fluorescence quantum yield increases 10–20 times. Moreover, the introduction of macrocycle into the molecule of **1a** suppresses noticeably the efficiency of radiationless deactivation. The formation of the RSS state is effectively suppressed in glassed matrices at 77 K, which manifests itself in a small Stokes shift under these conditions. Photorecoordination of metal cation is not suppressed even in rigid glassed matrices. However, the estimation of spectral properties of the metal complex **1b**·Ba^{2+} without photorecoordination may be carried out with the protonated product **1a**·H^{+}.

References

1. Volchkov VV, Uzhinov BM (2008) Structural relaxation of excited molecules of heteroaromatic compounds. High Energy Chem 42: 153–169
2. Grabowski ZR, Dobkowski J, Kühnle W (1984) Model compounds in study of the photophysical behaviour of carbonyl derivatives of N, N-dimethylaniline. J Mol Struct 114:93–100
3. Kummrow A, Dreyer J, Chudoba C, Stenger J, Nibbering ETJ, Elsaesser T (2000) Ultrafast charge transfer studied by femtosecond IR-spectroscopy and ab initio calculations. J Chin Chem Soc 47: 721–728
4. Maus M, Rettig W (2002) The excited state equilibrium between two rotational conformers of a sterically restricted donor-acceptor biphenyl as characterised by global fluorescence decay analysis. J Phys Chem A 106:2104–2111
5. Davis BN, Abelt CJ (2005) Synthesis and photophysical properties of models for twisted PRODAN and dimethylaminonaphthonitrile. J Phys Chem A 109:1295–1298
6. Zachariasse KA, Grobys M, von der Haar T, Hebecker A, Il'ichev YV, Morawski O, Rückert I, Kühnle W (1997) Photo-induced intramolecular charge transfer and internal conversion in molecules with a small energy gap between S_1 and S_2. Dynamics and structure. J Photochem Photobiol A Chem 105:373–383
7. Zachariasse KA, von der Haar T, Leinhos U, Kühnle W (1994) Solvent-induced pseudo-Jahn-Teller coupling in dual fluorescence evidence against the TICT hypothesis. J Inf Rec Mater 21:501–506
8. Lewis FD, Yang JS (1997) The excited state behavior of aminostilbenes. A new example of the meta effect. J Am Chem Soc 119:3834–3835
9. Kharlanov VA, Knyazhansky MI (1999) The dependence of photoinduced adiabatic transformations and fluorescence in 2,4,6-triarylsubstituted pyridinium cations on environment. J Photochem Photobiol A 125:21–27
10. Volchkov VV, Hue Bon Hoa G, Kossanyi JA, Gromov SP, Alfimov MV, Uzhinov BM (2005) Intramolecular structural relaxation in the excited hetarylazole cations. J Phys Org Chem 18:21–25
11. Volchkov VV, Khimich MN, Makarova NI, Uzhinov BM (2005) The dynamics of intramolecular excited state relaxation of N-anthryl substituted pyridinium cations. J Fluoresc 15:111–115
12. Doroshenko AO, Kirichenko AV, Mitina VG, Ponomaryev OA (1996) Spectral properties and dynamics of the excited state structural relaxation of the ortho analogues of POPOP. Effective abnormally large. Stokes shift luminophores. J Photochem Photobiol A 94:15–26
13. Al-Hassan KA (1995) Time-resolved fluorescence study of 4-dimethylaminobenzonitrile in nonhydrogen-bonding polymers, using picosecond dye laser pulses as excitation source. J Polym Sci B Polym Phys 33:725–730
14. Yguerabide J, Epstein HF, Stryer L (1970) Segmental flexibility in an antibody molecule. J Mol Biol 51:573–590
15. Nishimoto E, Yamashita S, Szabo ÄG, Imoto T (1998) Internal motions of lysozyme studies by time-resolved fluorescence depolarization of tryptophan residues. Biochemistry 37:5599–5607
16. Volchkov VV, Dem'yanov GV, Rusalov MV, Syreishchikova TI (2005) Fluorescence depolarization kinetics of neutral and charged 2-(3′-Pyridyl)oxazole. Russ J Gen Chem 75:790–794
17. Volchkov VV, Uzhinova LD, Uzhinov BM (2006) The dynamics of excited state structural relaxation of 4-dimethylaminobenzonitrile (DMABN) and related compounds. Int J Photoenergy 81896:1–6
18. Rechthaler K, Köhler G (1994) Excited state properties and deactivation pathways of 7-aminocoumarines. Chem Phys 189:99–116
19. Uzhinov BM, Ivanov VL, Melnikov MY (2011) Molecular rotors as luminescence sensors of local viscosity and viscous flow in solutions and organized systems. Russ Chem Rev 80:1179–1190
20. Loutfy RO, Law KY (1980) Electrochemistry and spectroscopy of intramolecular charge-transfer complexes. p-N, N-Dialkylaminobenzylidenemalononitriles. J Phys Chem 84:2803–2808
21. Even P, Chaubet F, Letourneur D, Viriot ML, Carré MC (2003) Coumarin-like fluorescent molecular rotors for bioactive polymers probing. Biorheology 40:261–263
22. Stsiapura VI, Maskevich AA, Kuzmitsky VA, Uversky VN, Kuznetsova IM, Turoverov KK (2008) Thioflavin T as a molecular rotor: Fluorescent properties of thioflavin T in solvents with different viscosity. J Phys Chem B 112:15893–15902
23. Singh PK, Kumbhakar M, Pal H, Nath S (2010) Viscosity effect on the ultrafast bond twisting dynamics in an amyloid fibril sensor: Thioflavin-T. J Phys Chem B 114:5920–5927
24. Hawe A, Filipe V, Jiskoot W (2010) Fluorescent molecular rotors as dyes to characterize polysorbate-containing IgG formulations. Pharm Res 27:314–326
25. Haidekker MA, Brady TP, Chalian SH, Akers W, Lichlyter D, Theodorakis EA (2004) Hydrophilic molecular rotor derivatives – synthesis and characterization. Bioorg Chem 32:274–289
26. Gromov SP (2008) Molecular meccano for light-sensitive and light-emitting nanosized systems based on unsaturated and macrocyclic compounds. Russ Chem Bull 57:1325–1350

27. Gromov SP, Ushakov EN, Vedernikov AI, Kuz'mina LG, Alfimov MV (2009) Molecular design of light-sensitive nanodimensional systems. Theor Exp Chem 45:3–11
28. Ushakov EN, Alfimov MV, Gromov SP (2008) Design principles for optical molecular sensors and photocontrolled receptors based on crown ethers. Russ Chem Rev 77:39–58
29. Gromov SP, Alfimov MV (1997) Supramolecular organic photochemistry of crown-ether-containing styryl dyes. Russ Chem Bull 46:611–636
30. Freeman HS, Peters AT (2000) Colorants for non-textile applications. Elsevier, Amsterdam
31. Aspland JR (1997) Textile dyeing and coloration. American association of textile chemists and colorists
32. Hunger K (2003) Industrial dyes: chemistry, properties, applications. Wiley-VCH, Weinheim
33. Strehmel B, Seifert H, Rettig W (1997) Photophysical properties of fluorescence probes. 2. A model of multiple fluorescence for stilbazolium dyes studied by global analysis and quantum chemical calculations. J Phys Chem B 101:2232–2243
34. Van der Meer MJ, Zhang H, Rettig W, Glasbeek M (2000) Femto and picosecond fluorescence studies of solvation and nonradiative deactivation of ionic styryl dyes in liquid solution. Chem Phys Lett 320:673–680
35. Thomas KJ, Thomas KG, Manojkumar TK, Das S, George MV (1994) Cation binding and photophysical properties of a monoaza-15-crown-5-ether linked cyanine dye. Proc Indian Acad Sci Chem Sci 106:1375–1383
36. Cao X, Tolbert RW, McHale JL, Edwards WD (1998) Theoretical study of solvent effects on the intramolecular charge transfer of a hemicyanine dye. J Phys Chem A 102:2739–2748
37. Shiraishi Y, Inoue T, Hirai T (2010) Local viscosity analysis of triblock copolymer micelle with cyanine dyes as a fluorescent probe. Langmuir 26:17505–17512
38. Wandelt B, Mielniczak A, Turkewitsch P, Darling GD, Stranix BR (2003) Substituted 4-[4-(dimethylamino)styryl]pyridinium salt as a fluorescent probe for cell microviscosity. Biosens Bioelectron 18: 465–471
39. Wandelt B, Cywinski P, Darling GD, Stranix BR (2005) Single cell measurement of micro-viscosity by ratio imaging of fluorescence of styrylpyridinium probe. Biosens Bioelectron 20:1728–1736
40. Reichardt C (2003) Solvents and solvent effects in organic chemistry, 3rd edn. Wiley-VCH Verlag GmbH & Co KGaA, Weinheim
41. Papper V, Pines D, Likhtenshtein G, Pines E (1997) Photophysical characterization of trans-4,4′-disubstituted stilbenes. J Photochem Photobiol A Chem 111:87–96
42. Gromov SP, Ushakov EN, Fedorova OA, Baskin II, Buevich AV, Andryukhina EN, Alfimov MV, Johnels D, Edlund UG, Whitesell JK, Fox MA (2003) Novel photoswitchable receptors: synthesis and cation-induced self-assembly into dimeric complexes leading to stereospecific [2+2]-photocycloaddition of styryl dyes containing a 15-Crown-5 ether unit. J Org Chem 68:6115–6125
43. Lednev IK, Ye TQ, Hester RE, Moore JN (1997) Photocontrol of cation complexation with a benzothiazolium styryl azacrown ether dye: spectroscopic studies on picosecond and kilosecond time scales. J Phys Chem A 101:4966–4972
44. Dumon P, Jonusauskas G, Dupuy F, Pee P, Rullière C, Létard JF, Lapouyade R (1994) Picosecond dynamics of cation-macrocycle interactions in the excited state of an intrinsic fluorescence probe: the calcium complex of 4-(*N*-Monoaza-15-crown-5)-4′-phenylstilbene. J Phys Chem 98:10391–10396
45. Yu J, Chen C, Chen Y (2011) Synthesis and fluorescent sensory properties of a 5-cyanostilbene derivative linked to monoaza-15-crown-5. J Taiwan Instit Chem Eng 42:674–681
46. Lippert E (1955) Dipolmoment und Elektronenstruktur von Angeregten Molekülen. Z Naturforsch A 10:541–545
47. Druzhinin SI, Rusalov MV, Uzhinov BM, Alfimov MV, Gromov SP, Fedorova OA (1995) Excited state relaxation processes of crowned styryl dyes and their metal complexes. Proc Indian Acad Sci Chem Sci 107:721–727
48. Gromov SP, Fedorova OA, Alfimov MV, Druzhinin SI, Rusalov MV, Uzhinov BM (1995) Crown-containing styryl dyes.14. Synthesis, luminescence, and complexation of the trans-isomers of chromogenic 15-crown-5-ethers. Russ Chem Bull 44:1922–1928
49. Freidzon AY, Bagatur'yants AA, Gromov SP, Alfimov MV (2003) Recoordination of a metal ion in the cavity of a crown compound: a theoretical study 1. Conformers of arylazacrown ethers and their complexes with Ca^{2+} cation. Russ Chem Bull 52:2646–2655
50. Freidzon AY, Bagatur'yants AA, Gromov SP, Alfimov MV (2005) Recoordination of a metal ion in the cavity of a crown compound: a theoretical study 2. Effect of the metal ion - solvent interaction on the conformations of calcium complexes of arylazacrown ethers. Russ Chem Bull 54:2042–2054
51. Freidzon AY, Bagatur'yants AA, Gromov SP, Alfimov MV (2008) Recoordination of a metal ion in the cavity of a crown compound: a theoretical study 3. Absorption spectra and excited states of azacrown-containing styryl dyes and their complexes. Russ Chem Bull 57:2045–2055
52. Freidzon AY, Bagatur'yants AA, Ushakov EN, Gromov SP, Alfimov MV (2011) Ab initio study of the structure, spectral, ionochromic, and fluorochromic properties of benzoazacrown-containing dyes as potential optical molecular sensors. Int J Quantum Chem 111:2649–2662
53. Rusalov MV, Uzhinov BM, Alfimov MV, Gromov SP (2010) Photoinduced recoorodination of metal cations in complexes with chromogenic crown ethers. Russ Chem Bull 79:1099–1121
54. Druzhinin SI, Rusalov MV, Uzhinov BM, Gromov SP, Sergeev SA, Alfimov MV (1999) Fluorescence of crowned butadienyl dye and its metal complexes. J Fluoresc 9:33–36
55. Nasimova IR, Ushakov EN, Makhaeva EE, Fedorova OA, Gromov SP, Alfimov MV, Khokhlov AR (2002) Effect of a polymer matrix on the complexation and photochemical behavior of an azacrown-containing styryl dye. Polym Sci A 44:1313–1318
56. Brearley AM, Flom SR, Nagarajan V, Barbara PF (1986) Dynamic solvent effects on large-amplitude isomerization rates 2. 2-(2′-propenyl)anthracene and (E)-2-(but-2′-en-2′-yl)anthracene. J Phys Chem 90:2092–2099
57. Hicks JM, Vandersall MT, Sitzmann EV, Eisenthal KB (1987) Polarity-dependent barriers and the photoisomerization dynamics of molecules in solution. Chem Phys Lett 135:413–420
58. Alkindi AS, Al-Wahaibi YM, Muggeridge AH (2008) Physical properties (Density, excess molar volume, viscosity, surface tension, and refractive index) of ethanol+glycerol. J Chem Eng Data 53:2793–2796
59. Vedernikov AI, Kuz'mina LG, Sazonov SK, Lobova NA, Loginov PS, Churakov AV, Strelenko YA, Howard JAK, Alfimov MV, Gromov SP (2007) Styryl dyes. Synthesis and study of the solid state [2+2] autophotocycloaddition by NMR spectroscopy and X-ray diffraction. Russ Chem Bull Int Ed 56:1860–1883
60. Atabekyan LS, Vedernikov AI, Avakyan VG, Lobova NA, Gromov SP, Chibisov AK (2013) Photoprocesses in styryl dyes and their pseudorotaxane complexes with cucurbit[7]uril. J Photochem Photobio A 253:52–61
61. Brouwer AM (2011) Standards for photoluminescence quantum yield measurements in solution. Pure Appl Chem 83:2213–2228
62. Melhuish WH (1961) Quantum efficiencies of fluorescence of organic substances: effect of solvent and concentration of the fluorescence solute. J Phys Chem 65:229–235